International Journal of Scientific Research in Computer Science, Engineering and Information Technology
ISSN : 2456-3307 (www.ijsrcseit.com)
doi : https://doi.org/10.32628/CSEIT2390140

Maize Disease Detection using Color Cooccurrence Features

Esmael Ahmed, Kedir Abdu
Department of Information System, Wollo University, Dessie, Ethiopia

ARTICLEINFO

Article History:

Accepted: 15 Feb 2023
Published: 05 March 2023

Publication Issue
Volume 10, Issue 2
March-April-2023

Page Number
01-10

ABSTRACT

The Ethiopian economy is based primarily on agriculture. Furthermore, due to Ethiopia's predominately agricultural economy, most Ethiopians are dependent on agriculture in some way. In Ethiopia, traditional dishes including bread, injera, and soup are commonly made from one of the plants, maize. Although growing maize, Wollo farmers experience low levels of yield due to a variety of problems. This study examines the features of color co-occurrence to identify Maize illness. Although it has not been proven, several diseases may occur in Ethiopia. In this research features from the images are retrieved, while the texture feature from the color co-occurrence matrix is used. Artificial Neural Networks and Leaf Color Analysis are used to categorize the diseases classified as Maize Blast, Brown Spot, Narrow Spot, and Normal Maize Leaf. Analyze and classify the Maize disease, the process entails acquiring, evaluating, and classifying images. The entire Maize sample goes through the leaf color analysis before moving on to the artificial neural network.. All samples are subjected to a leaf color analysis throughout the testing step in order to identify the leaf diseases. If the sample's RGB values fall within a predetermined range, it is automatically classified as a normal Maize leaf; nevertheless, all diseased samples undergo image processing in order to get the features that utilized to train and evaluate an artificial neural network. The generated model is then discovered when an artificial neural network is trained using these features. As a result, the artificial neural network technique is used to identify the Maize diseases with an accuracy rate of roughly 86%.

Keywords - Plant Disease Detection; Color Co-occurrence Features.

I. INTRODUCTION

For emerging nations to have economic progress, the agriculture sector is crucial. The Ethiopian economy is regarded as having its foundation in agriculture. In 2019, the GDP contribution from agriculture was roughly 34%, and 90% of Ethiopia's population is either directly or indirectly reliant on the sector [1]. Native Americans improved the crop Maize, which they developed from a wild grass in Mexico 7000

years ago, to make it a more nutritious food source [2]. Recently, Maize is grown throughout the world, United States, China, and Brazil being the top three Maize-producing countries in the world [2]. Maize is also a substantial component of the diet of approximately 85% of Ethiopia's population. The Maize is said to have travelled from Kenya to Ethiopia. In recent years, Maize has become Ethiopia's most important grain crop [3]. Ethiopia is the second highest Maize producer in Sub-Saharan Africa next to Nigeria [3]. Maize production of Ethiopia increased from 939 thousand tonnes in 1970 to 8500 thousand tonnes in 2019, growing at annual rate 7.64% [4]. Similarly, the Maize production increased from 8350 thousand tonnes in 2018 to 8500 thousand tonnes in 2019 with growing annul rate 1.8% [4]. It has been reported that a lot of households now grow Maize than any other cereal in Ethiopia [4]. Maize is an agricultural product in most of the Ethiopia regions like the Amhara, the Oromia and the south nation and nation and national states [5].

Humans must prioritize the prevention of plant diseases because they harm the plants and plant products that provide them with food, clothing, furniture, the environment, and frequently even their homes [6]. Plant diseases cause different types and sizes of losses depending on the plant or plant products, the pathogen, the location, the environment, the control techniques utilized, and combinations of these factors [6]. One of the main biotic restrictions on crop output and product quality that ultimately drives down market prices is disease. The attack of numerous plant diseases at various phases of crop development is the cause of the low production of the majority of the crops in Ethiopia [7].

The majority of Maize farmers encounter numerous difficulties during Maize harvest because they frequently contract bacterial and fungal diseases. Additionally, when the Maize was harmed or diseased, the other parts were exposed to infection [8]. As a result, Maize farmers earn less money and suffer significant losses. The type of illness is currently determined manually by the Maize grower. Errors could occur when attempting to categorize diseases [8]. Additionally, it takes a lot of time for Maize farmers to identify the illness. Since the Maize field is large, it also takes time for the Maize growers to manually inspect it for disease. Therefore, this study aims to develop a prototype system to automatically detect and classify the Maize diseases by using image processing technique.

II. METHODS AND MATERIAL

As a result, Maize farmers earn less money and suffer significant losses. The type of illness is currently determined manually by the Maize grower. Errors could occur when attempting to categorize diseases. Additionally, it takes a lot of time for Maize farmers to identify the illness. Since the Maize field is large, it also takes time for the Maize growers to manually inspect it for disease [9]. Because watching the co-occurrence of two occurrences is significantly more informative than observing the occurrence of each event separately, co-occurrence characteristics are effective for classifying objects [10]. Therefore, in this study we have used color Co-occurrence features to Maize disease detection.

A. Work Flow

The work flow in this research has been generalized as follow in Figure 1:

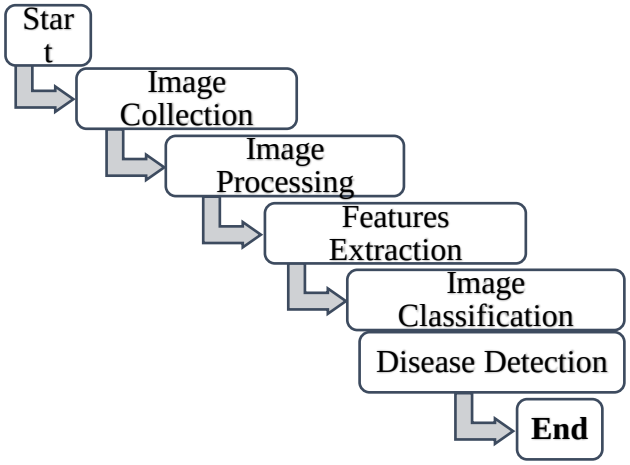

Figure 1. Work Flow of proposed methodology

B. Image Collection

Maize leaf RGB images have been gathered from Ministry of Agriculture portal. These images were reduced in size to 64 × 64 pixels and used as training data. With the four rotations from each image, we obtain roughly 180 data samples. There are three different varieties of Maize diseases (Blast, Brown Spot, Narrow Brown Spot).

(a) (b) (c)

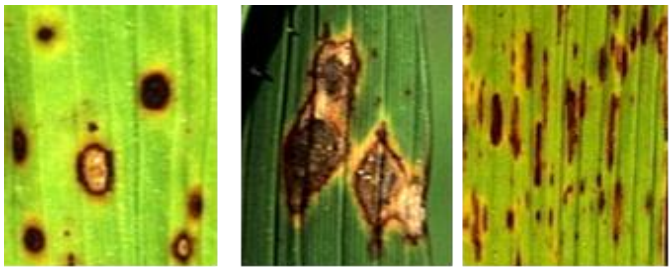

Figure 2 Sample of collected images (a) Brown Spot Disease; (b) Narrow Brown Spot Disease (c) Blast Disease

C. Image Processing

The basic goal of this procedure is to produce an image that closely resembles how people see color. The RGB image is transformed into Lab using the CIEL*a*b* 1976 color space as the acronym (also CIELAB). A three-axis color system, the LAB color model is absolute, which means that the color is precise. Device independence means that the only way to convey different colors between various devices is through the LAB color space. An object's color is measured in LAB color with a Spectro image meter. Figure 3 shows color space in dimensional graph.

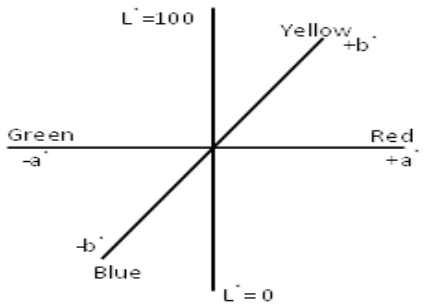

Figure 3 L*a*b* Color Space in Dimensional Graph

These three coordinates of CIELAB represent-

- The lightness of the color L* = 0 yields black and L* = 100 indicates diffuse white; specular white may be higher
- Its position between red/magenta and green (a*, negative values indicate green while positive values indicate magenta) and
- Its position between yellow and blue (b*, negative values indicate blue and positive values indicate yellow).

(a) (b)

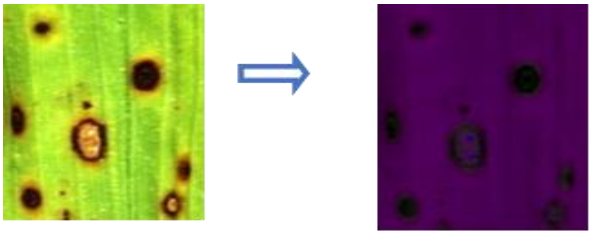

Figure 4 Processing image from RGB to Lab (a) RGB image; (b) Lab image

D. Feature Extraction

Feature extraction a sort of dimensionality lessening that productively speaks to intriguing parts of a image as a smaller component vector. Features are extracted from the color co-occurrence matrix which is calculated previously.

E. Color Co-occurrence Matrix

A co-occurrence matrix or co-occurrence distribution is a matrix that is defined over an image to be the distribution of co-occurring pixel values (grayscale values, or colors) at a given offset [11]. The offset, is a position operator that can be applied to any pixel in the image (ignoring edge effects): An image with different pixel values will produce a co-occurrence matrix, for the given offset. The value of the co-occurrence matrix gives the number of times in the image that the and pixel values occur in the relation given by the offset [11].

Where: i and j are the pixel values; x and y are the spatial positions in the image I; the offsets $(\Delta x, \Delta y)$ define the spatial relation for which this matrix is

calculated; and $I(\Delta x, \Delta y)$ indicates the pixel value at pixel (x, y).

The offset value $(\Delta x, \Delta y)$ is calculated by the spatial direction. If the direction is

$0°$, then $\Delta x = 0,\ \Delta y = 1$
$45°$, then $\Delta x = 1,\ \Delta y = 1$
$90°$, then $\Delta x = 1,\ \Delta y = 0$
$135°$, then $\Delta x = -1,\ \Delta y = 1$

Let's take an example of an $5x5$ image and the GLCM matrix is calculated by following procedure:

$$\begin{bmatrix} 22 & 220 & 180 & 111 & 75 \\ 25 & 240 & 103 & 180 & 118 \\ 65 & 110 & 210 & 230 & 191 \\ 123 & 40 & 150 & 5 & 199 \\ 180 & 95 & 70 & 15 & 255 \end{bmatrix}$$

The matrix size is $5x5$. So, the segment size will be $255/5 = 51$ and all values of the above matrix will be replaced by below:

$$0 - 51 \rightarrow 0$$
$$52 - 103 \rightarrow 1$$
$$104 - 154 \rightarrow 2$$
$$155 - 205 \rightarrow 3$$
$$206 - 255 \rightarrow 4$$

By applying above mapping the resultant matrix is given below:

$$\begin{bmatrix} 0 & 4 & 3 & 2 & 1 \\ 0 & 4 & 1 & 3 & 2 \\ 1 & 2 & 4 & 4 & 3 \\ 2 & 0 & 2 & 0 & 3 \\ 3 & 1 & 1 & 0 & 4 \end{bmatrix}$$

When the direction is $0°$ and the offset value is 1, then the matrix which will be found is given below:

$$\begin{bmatrix} 0 & 0 & 1 & 1 & 3 \\ 1 & 1 & 1 & 1 & 0 \\ 2 & 1 & 0 & 0 & 1 \\ 0 & 1 & 2 & 0 & 0 \\ 0 & 1 & 0 & 2 & 1 \end{bmatrix}$$

The transpose matrix of the above matrix is given below:

$$\begin{bmatrix} 0 & 1 & 2 & 0 & 0 \\ 0 & 1 & 1 & 1 & 1 \\ 1 & 1 & 0 & 2 & 0 \\ 1 & 1 & 0 & 0 & 2 \\ 3 & 0 & 1 & 0 & 1 \end{bmatrix}$$

After Adding the above two matrices, we get the following matrix:

$$\begin{bmatrix} 0 & 1 & 3 & 1 & 3 \\ 1 & 2 & 2 & 2 & 1 \\ 3 & 2 & 0 & 2 & 1 \\ 1 & 2 & 2 & 0 & 2 \\ 3 & 1 & 1 & 2 & 2 \end{bmatrix}$$

Now, the determinant of this matrix = 40. By normalizing the matrix, we get resultant matrix:

$$\begin{bmatrix} 0 & 0.025 & 0.075 & 0.025 & 0.075 \\ 0.025 & 0.050 & 0.050 & 0.050 & 0.025 \\ 0.075 & 0.050 & 0 & 0.050 & 0.025 \\ 0.025 & 0.050 & 0.050 & 0 & 0.050 \\ 0.075 & 0.025 & 0.025 & 0.050 & 0.050 \end{bmatrix}$$

This is the resultant GLCM matrix when the offset value is 1 and rotation is$0°$. Therefore, we apply CCM in the figure 5 image of size 64 x 64, a 20 x 20 CCM matrix will be found. Figure5 depicts Brown Spot affected Maize image.

Figure 5 Brown Spot affected Maize image

F. Textural Features

Notations:

$p(i,j)$ (i,j)th entry in the normalized gray level co-occurrence matrix

$p_x(i)$ ith entry in the marginal probability matrix obtained by summing the rows of $p(i,j)$

N_g number of distinct gray levels in the quantized image.

1) Angular Second Moment [12]:

$$f_1 = \sum_i \sum_j (p(i,j)^2) \qquad (1)$$

Angular Second Moment measure the smoothness of the image using Equation 1 formulas [12]. There are two cases,

If all pixels have same gray level I=k,

$p(k,k) = 1$ if $(i = j)$ and $p(i,j) = 0$ if otherwise.

$ASM = 1$

If all pixels have different gray level,

$p(i,j) = {}^{1}/_{R}$ & $ASM = {}^{1}/_{R}$

ASM value of figure 5 image is: 0.00528

2) Contrast [13]:

$$f_2 = \sum_{n=0}^{N_g-1} n^2 \left\{\sum_{i=1}^{N_g} \sum_{j=1}^{N_g} p(i,j)\right\} \quad (2)$$

Contrast measures the image contrast [13] (locally gray level variations) as shown in Equation 2. The term n^2 is used to take of the largest contrast value.

Contrast value figure 5 image is: 26.67

3) Correlation [14]:

$$f_3 = \frac{\sum_i \sum_j (ij)p(i,j) - \mu_x \mu_y}{\sigma_x \sigma_y} \quad (3)$$

Equation 3 shows correlation [14] which measures how the pixels are correlated with each other. Where μ_x, μ_y are the standard deviations and σ_x, σ_y are means of p_x, p_y

Correlation value of figure 5 image is: 0.557

4) Sum of squares: Variance [15]

$$f_4 = \sum_i \sum_j (i-\mu)^2 p(i,j) \quad (4)$$

Sum of squares value of figure 5 image is: 128.231

5) Inverse Difference Moment(Homogeneity) [16]

$$f_5 = \sum_i \sum_j \frac{1}{1+(i-j)^2} p(i,j) \quad (5)$$

Inverse Difference Moment takes care of low contrast images. It takes care of low contrast images because of the inverse $(i-j)^2$.

Homogeneity value of figure 5 image is: 0.30597

6) Sum Average [17]:

$$f_6 = \sum_{i=2}^{2N_g} i p_{x+y}(i) \quad (6)$$

Sum Average value of figure 5 image is: 19.807

7) Sum Variance [17]:

$$f_6 = \sum_{i=2}^{2N_g} (i - f_8)^2 p_{x+y}(i) \quad (7)$$

Sum Variance value of figure 5 image is: 426.844

8) Sum Entropy [18]:

$$f_8 = -\sum_{i=2}^{2N_g} p_{x+y}(i) log\{p_{x+y}(i)\} \quad (8)$$

Sum Entropy value of figure 5 image is: 1.554

9) Entropy [19]

$$f_9 = -\sum_i \sum_j p(i,j) log\{p(i,j)\} \quad (9)$$

Entropy [19] takes low values for smooth images. It measures the randomness.

Entropy value of figure 5 image is: 2.4052

10) Difference Variance [20]

$$f_{10} = variance\ of\ p_{x-y} \quad (10)$$

Difference Variance value of figure 5 image is: 0.00436

11) Difference Entropy shown in Equation 11.

$$f_{11} = -\sum_{i=0}^{N_g-1} p_{x-y}(i)\ log\{p_{x-y}(i)\} \quad (11)$$

Difference Entropy value of figure 5 image is: 0.99

12) Information Measure [21]of Correction calculated using Equation 12, 13 and 14.

$$f_{12} = \frac{HXY - HXY1}{max\{HX, HY\}} \quad (12)$$

$$f_{13} = (1 - exp[-2.0(HXY2 - HXY)])^{1/2} \quad (13)$$

$$HXY = -\sum_i \sum_j p(i) log\{p(i)\} \quad (14)$$

Since some of the probabilities becomes zero and $log(0)$ is very high so arbitrary small positive constant is added to avoid the infinite number [21]. Equation 15 and 16 shows the formula to avoid the infinite number.

Where, HX and HY are entropies of p_x and p_y and

$$HXY1 = -\sum_i \sum_j p(i,j) log\{p_x(i)p_y(j)\} \quad (15)$$

$$HXY2 = -\sum_i \sum_j p_x(i)p_y(j) log\{p_x(i)p_y(j)\} \quad (16)$$

Information Measure of Correlation 1 value of figure 5 image is: -0.1358

Information Measure of Correlation 2 value of figure 5 image is: 0.4915

13) Maximal Correction Coefficient (Energy) [22]. Equation 17 and 18 shows correlation coefficient and energy respectively.

$$f_{14} = (second\ largest\ eigenvalue\ of\ Q)^{1/2} \quad (17)$$

Where,

$$Q(i,j) = \sum_k \frac{p(i,k)p(j,k)}{p_x(i)p_y(k)} \quad (18)$$

Energy value of figure 5 image is: 0.0711

G. Feature Selection

A crucial problem for the system is choosing the appropriate features. Not all features are appropriate for categorizing the various classes. Only 5 of the 14

features we examined in our study are appropriate, we discovered. A technique known as the Subset Choosing Method is utilized to choose those traits.

The methodology is:

```
ans = 0.0
subset = 1
for i in range (1, (1<<15)):
ret = fun(i)
if (ret>ans):
ans = ret
subset = i
```

There are possible subsets among them the subset which is the possible best subset. So, the selected features are:

- Homogeneity
- Angular Second Moment (ASM)
- Energy
- Information Measure of Correlation 1
- Information Measure of Correlation 2

H. Classification

A classifier is now required to classify the images after the features from the images have been extracted. As a classifier in this instance, an artificial neural network with three hidden layers is utilized. There are two steps in the classifier. A classifier algorithm will be employed to find the diseases if an image fails leaf color analysis.

i. Leaf Color Analysis

First the whole image is scanned through and calculates the minimum and maximum value for each channel. The RGB calculation will be passed. Equation 19, 20 and 21 shows R, G and B calculation respectively.

$$93 \leq R_{min} \leq 211 \;\&\; 93 \leq R_{max} \leq 211 \quad (19)$$

$$142 \leq G_{min} \leq 222 \;\&\; 142 \leq G_{max} \leq 222 \quad (20)$$

$$64 \leq B_{min} \leq 155 \;\&\; 64 \leq B_{max} \leq 155 \quad (21)$$

An image is considered to be a typical leaf image if it meets all of the aforementioned requirements. If not, it is a compromised image. We used several typical images of Maize leaves to generate the histogram values before calculating those values. The minimum and maximum values from those histogram values were computed.

I. Artificial Neural Network

All the selected features are in the input of an Artificial Neural Network and the output is used in classification. The equation which is minimized is

$$WX + B$$

Where,

$$W = weights$$

$$B = biases$$

$$X = Input\ Features$$

The aforementioned equation is reduced to ensure that the cost function has the smallest potential inaccuracy. There are nodes and edges connecting the nodes in an artificial neural network. The nodes indicate various activation functions, whereas the edges represent various arbitrary values. Tensor Flow is employed as the deep learning framework in our suggested methodology. TensorFlow is a typical computational network that may be used to carry out calculations much more quickly than if they were done directly in Python. TensorFlow can be more effective than NumPy because it is aware of the full computation graph that has to be performed, whereas NumPy is only aware of doing a single mathematical operation at a time. In order to improve the performance of the model, TensorFlow may also automatically calculate the gradients required to optimize the graph's variables. This is so because the graph is made up of a series of straightforward equations. Consequently, the iterative chain rule method can be used to calculate the gradient of the entire graph.

Figure 6 shows our used system, where the network architecture 15 – 50 – 50 – 50 – 4 nodes in 1 input, 3 hidden and 1 output layer respectively. It is a fully connected artificial neural network. Each hidden layer has 50 nodes which gives better result in our research. The hidden nodes are chosen by comparative study.

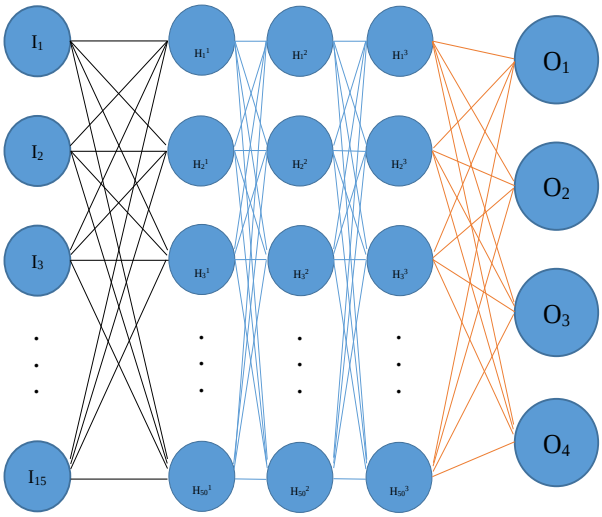

Figure 6. The Proposed Artificial Neural Network

J. Performance Measures

In this work, the effectiveness of a categorization strategy was summarized using a confusion matrix. When there are more than two classes in a dataset or when there are not an equal number of observations in each class, classification accuracy might be deceptive. Confusion matrix calculation provides a clearer image of the classification model's successes and shortcomings.

The easiest performance metric to understand is accuracy, which is just the proportion of properly predicted observations to all observations [23]. Therefore, one has to look at other parameters to evaluate the performance of the model [23]. Equation 22 shows formula of accuracy.

$$Accuracy = \frac{TP+TN}{TP+FP+TN+FN} \quad (22)$$

Precision is the ratio of correctly predicted positive observations to the total predicted positive observations [24]. The question that this metric answer is of all passengers that labeled as survived, how many actually survived? High precision relates to the low false positive rate.

$$Precision = \frac{TP}{TP+FP} \quad (23)$$

Recall is the ratio of correctly predicted positive observations to the all observations in actual class – yes [25]. The question recall answers, is: Of all the leaves that truly are in this particular class, how many did we label [25].

$$Recall = \frac{TP}{TP+FN} \quad (24)$$

III.RESULTS AND DISCUSSION

There are 220 samples of Maize image used as sample data in the testing phase of this development. The Maize images samples had gone through the phases as discus in the above section. The experiments and analysis processes are done on a computer with Core-I5 processor having 4 cores with each core having 2.5GHz Speed. Also, the system had 4GB of RAM, and 1GB of internal intel HD video memory. For software, PyCharm Community Edition 2017.1 is used and program is done with python language with OpenCV and deep learning framework, TensorFlow. OpenCV (Open-Source Computer Vision) is a library of programming functions mainly aimed at real-time computer vision. The reason for using OpenCV because it gives easy functionality to do different processes without going into implementations.

Maize Blast, Brown Spot, Narrow Brown Spot, and Other, four classes, should be indicated as PB, BS, NBS, and O, respectively. Predicted class and actual class are displayed in column and row, respectively. As a result, table 2 shows matrix of confusion as follows:

Table 1. Confusion matrix of proposed system

		Predicted Class			
		PB	BS	NBS	O
Actual Class	PB	17	1	0	1
	BS	0	13	0	1
	NBS	0	1	7	1
	O	1	0	1	3

Random test is used to determine the robustness of a system. Here all the data are taken and from the data randomly some data are selected for testing and some data are selected for training. Here k-fold means, the whole data are divided into k-fold, and then each fold

is used as testing data and rest of the data are used as training data. And there is n-number of runs. 5-fold is used within 3 distinct run with our collected data and the resulted values are showed in the table 2 with the accuracy, precision and recall individually, as average and total.

Table 2. Accuracy, Precision and Recall with k-fold(5-fold) method

Run	Fold	Fold Accuracy(%)	Fold Precision(%)	Fold Recall(%)	Run Accuracy(%)	Run Precision(%)	Run Recall(%)	Total Accuracy(%)	Total Precision(%)	Total Recall(%)
1	1	86.4	90.3	73.8	86.38	87.52	80.02	85.69	83.36	76.17
	2	84.1	85.6	78.3						
	3	81.8	78.9	83.3						
	4	93.2	94.2	88.0						
	5	86.4	88.6	76.7						
2	1	84.1	73.4	75.0	84.38	78.72	73.28			
	2	86.4	66.9	70.3						
	3	90.0	92.4	80.5						
	4	77.3	78.3	63.6						
	5	84.1	82.0	77.0						
3	1	79.5	76.7	68.9	86.32	84.74	75.2			
	2	86.3	89.6	74.4						
	3	88.6	89.8	73.9						
	4	88.6	91.3	81.2						
	5	88.6	76.3	77.6						

Total 87 leaves which are affected by Maize Blast disease are used for experiment. In those leaves, 10 images were misclassified and the other 77 images are correctly classified as Maize Blast. Accuracy of Maize Blast is 88.51%.

Examples: Correctly classified

Figure 7 Correctly classified 4 Maize Blast images

Incorrectly classified

Figure 8 Incorrectly classified 4 Maize Blast images

Total 56 leaves which are affected by Maize Blast disease are used for experiment. In those leaves, 14 images were misclassified and the other 42 images are correctly classified as Brown Spot. Accuracy of Brown Spot is 75.00%.

Examples: Correctly classified

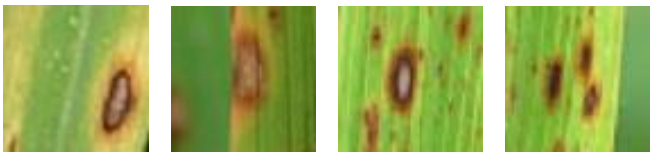

Figure 9 correctly classified 4 Brown Spot images

Incorrectly classified

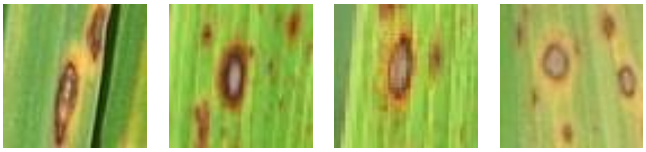

Figure 10 Incorrectly classified 4 Brown Spot images

Total 33 leaves which are affected by Maize Blast disease are used for experiment. In those leaves, 4 images were misclassified and the other 29 images are correctly classified as Narrow Brown Spot. Accuracy of Narrow Brown Spot is 87.87%.

Examples: Correctly classified

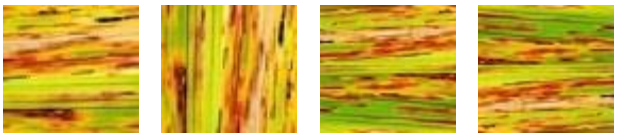

Figure 11 Correctly classified 4 Narrow Brown Spot images

Incorrectly classified

Figure 12 Incorrectly classified 4 Narrow Brown Spot images

IV.CONCLUSION

In this study the impact of color co-occurrence features in the detection of Maize disease has been

investigated. The Python application was used to create the suggested system for diagnosing Maize disease. Image processing techniques are used to enhance and increase the image's quality. In addition, the Maize blast, Brown Spot, Narrow Spot, and Normal Maize Leaf illnesses are classified using Artificial Neural Networks and Leaf Color Analysis. The methodology involves gathering, analysing, and classifying images for use in analysis and categorization of the Maize disease. Before moving on to the artificial neural network, the full Maize sample will pass through the analysis of the leaf color. The sample is automatically classified as a normal Maize leaf if its RGB values fall within a certain range, but all disease-affected samples must go through image processing to obtain the characteristics that will be used to train and test an artificial neural network. Consequently, the Maize illnesses are identified with an accuracy rate of roughly 86% when using the artificial neural network technique. There is a very high chance that this study will be significantly enhanced in the future. There aren't many obstacles to our suggested course of action. The accuracy percentage is one of them. The accuracy rate of 86% is not high enough. This number has to be increased for better results. There could be implementation errors as well. Because choosing the best features is a time-consuming and difficult computational procedure, we were unable to check every conceivable feature subset. Based on prior best features, we merely checked a few random features. There is a chance that some of the better features will disappear. Additionally, because it takes so much time, our implementation is a little slower. As a result, it cannot yet be used in real time.

Even though we made every effort to achieve the intended result and this method's accuracy value is fairly good, there is still room for development as long as it is not quite 100%. This method can be made to operate in real time by employing a more effective method to select the finest features. can be used in LBP, which might improve accuracy. Implementing a mobile application will make it possible for farmers to quickly identify the disease before it is too late.

Conflicts of Interest

The authors declare that there is no conflict of interest regarding the publication of this paper.

Funding Statement

This research received no specific grant from any funding agency in the public, commercial, or not-for-profit sectors.

V. REFERENCES

[1]. Y. Alemu and D. Tolossa, “Livelihood impacts of large-scale agricultural investments using empirical evidence from shashamane rural district of oromia region, Ethiopia,” Sustainability, vol. 14, no. 15, p. 9082, 2022.

[2]. P. Ranum, J. P. Peña-Rosas, and M. N. Garcia-Casal, “Global maize production, utilization, and consumption,” Ann. N. Y. Acad. Sci., vol. 1312, no. 1, pp. 105–112, 2014.

[3]. J. Bellarby et al., “Identifying secure and low carbon food production practices: A case study in Kenya and Ethiopia,” Agric. Ecosyst. \& Environ., vol. 197, pp. 137–146, 2014.

[4]. A. B. Eticha, “Contributing factors of maize production using multiple linear regressions in mizan-aman district, bench-shako zone, Southwest of Ethiopia,” Open J. Plant Sci., vol. 5, no. 1, pp. 40–45, 2020.

[5]. T. Abate et al., “Factors that transformed maize productivity in Ethiopia,” Food Secur., vol. 7, no. 5, pp. 965–981, 2015.

[6]. G. N. Agrios, Plant pathology. Elsevier, 2005.

[7]. M. BERHAN and D. BEKELE, “REVIEW OF MAJOR CEREAL CROPS PRODUCTION LOSSES, QUALITY DETERIORATION OF GRAINS BY WEEDS AND ITS PREVENTION IN ETHIOPIA,” Asian J. Adv. Res., pp. 93–104, 2021.

[8]. A. J. Ullstrup, “The impacts of the southern corn leaf blight epidemics of 1970-1971,” Annu. Rev. Phytopathol., vol. 10, no. 1, pp. 37–50, 1972.

[9]. M. Haque et al., "Deep learning-based approach for identification of diseases of maize crop," Sci. Rep., vol. 12, no. 1, pp. 1–14, 2022.

[10]. L. D. Paccola-Meirelles, A. S. Ferreira, W. F. Meirelles, I. E. Marriel, C. R. Casela, and others, "Detection of a bacterium associated with a leaf spot disease of maize in Brazil.," J. Phytopathol., vol. 149, no. 5, pp. 275–279, 2001.

[11]. J.-J. Qiu, Y. Wu, B. Hui, J. Chen, L. Ji, and M. Wang, "A novel texture analysis method based on reverse biorthogonal wavelet and co-occurrence matrix applied for classification of hepatocellular carcinoma and hepatic hemangioma," J. Med. Imaging Heal. Informatics, vol. 8, no. 9, pp. 1835–1843, 2018.

[12]. M. Stankovic et al., "Quantification of structural changes in acute inflammation by fractal dimension, angular second moment and correlation," J. Microsc., vol. 261, no. 3, pp. 277–284, 2016.

[13]. D. Vijayalakshmi, M. K. Nath, and O. P. Acharya, "A comprehensive survey on image contrast enhancement techniques in spatial domain," Sens. Imaging, vol. 21, no. 1, p. 40, 2020.

[14]. E. Grunwald and S. Winstein, "The correlation of solvolysis rates," J. Am. Chem. Soc., vol. 70, no. 2, pp. 846–854, 1948.

[15]. C. Inclan and G. C. Tiao, "Use of cumulative sums of squares for retrospective detection of changes of variance," J. Am. Stat. Assoc., vol. 89, no. 427, pp. 913–923, 1994.

[16]. T. Mapayi, S. Viriri, and J.-R. Tapamo, "A new adaptive thresholding technique for retinal vessel segmentation based on local homogeneity information," in Image and Signal Processing: 6th International Conference, ICISP 2014, Cherbourg, France, June 30--July 2, 2014. Proceedings 6, 2014, pp. 558–567.

[17]. N. Abbas, M. Riaz, and R. J. M. M. Does, "Mixed exponentially weighted moving average--cumulative sum charts for process monitoring," Qual. Reliab. Eng. Int., vol. 29, no. 3, pp. 345–356, 2013.

[18]. N. L. Guevara, R. P. Sagar, and R. O. Esquivel, "Shannon-information entropy sum as a correlation measure in atomic systems," Phys. Rev. A, vol. 67, no. 1, p. 12507, 2003.

[19]. A. Wehrl, "General properties of entropy," Rev. Mod. Phys., vol. 50, no. 2, p. 221, 1978.

[20]. H. Scheffe, The analysis of variance, vol. 72. John Wiley \& Sons, 1999.

[21]. N. X. Vinh, J. Epps, and J. Bailey, "Information theoretic measures for clusterings comparison: is a correction for chance necessary?," in Proceedings of the 26th annual international conference on machine learning, 2009, pp. 1073–1080.

[22]. W. Bryc and A. Dembo, "On the maximum correlation coefficient," Theory Probab. \& Its Appl., vol. 49, no. 1, pp. 132–138, 2005.

[23]. R. C. Fair, "Evaluating the predictive accuracy of models," Handb. Econom., vol. 3, pp. 1979–1995, 1986.

[24]. T. Kynkäänniemi, T. Karras, S. Laine, J. Lehtinen, and T. Aila, "Improved precision and recall metric for assessing generative models," Adv. Neural Inf. Process. Syst., vol. 32, 2019.

[25]. A. Lavie, K. Sagae, and S. Jayaraman, "The significance of recall in automatic metrics for MT evaluation," in Machine Translation: From Real Users to Research: 6th Conference of the Association for Machine Translation in the Americas, AMTA 2004, Washington, DC, USA, September 28-October 2, 2004. Proceedings 6, 2004, pp. 134–143.

Cite this article as :

Esmael Ahmed, Kedir Abdu, "Maize Disease Detection using Color Cooccurrence Features", International Journal of Scientific Research in Computer Science, Engineering and Information Technology (IJSRCSEIT), ISSN : 2456-3307, Volume 9, Issue 2, pp.01-10, March-April-2023. Available at doi :

https://doi.org/10.32628/CSEIT2390140

Journal URL : https://ijsrcseit.com/CSEIT2390140